Macromolecular Research, Vol. 22, No. 1, pp 47-57 (2014)
DOI 10.1007/s13233-014-2002-4

www.springer.com/13233
pISSN 1598-5032 eISSN 2092-7673

In vitro Micro-Mineralized Tissue Formation by the Combinatory Condition of Adipose-Derived Stem Cells, Macroporous PLGA Microspheres and a Bioreactor

Min-Seo Jung[1], Han Byul Jang[2], Soo-Eon Lee[2], Jae-Hong Park[2], and Yu-Shik Hwang*[,1]

[1]*Department of Maxillofacial Biomedical Engineering and Institute of Oral Biology, Kyung Hee University, Seoul 130-701, Korea*
[2]*Department of Pediatric Dentistry, School of Dentistry, Kyung Hee University, Seoul 130-701, Korea*

Received May 28, 2013; Revised July 16, 2013; Accepted July 25, 2013

Abstract: For the final purpose of accelerating the restoration of defected bone tissue, researches for developing *in vitro* three dimensional (3D) mineralized tissue using various stem cells, scaffolds and culture systems have been extensively done. In this research, an integrated bioprocess to generate stem cell-based 3D mineralized construct was developed using adipose-derived stem cell (ADSC), highly porous biodegradable poly(*D*,*L*-lactide-*co*-glycolide) (PLGA) microspheres and a high-aspect ratio vessel (HARV) bioreactor system. First, ADSCs adhered uniformly on poly-*L*-ornithine-coated macroporous PLGA microspheres, and the ADSC/microsphere composites were cultured in the presence of osteogenic supplements in a HARV bioreactor. Alkaline phosphatase (ALPase) activity assay, immunocytochemical staining and quantitative real-time polymerase chain reaction (qPCR) analysis showed temporal increase of ALPase activity, molecular expressions of type I collagen, osteocalcin and runx2 and upregulation of runx2, Sp7, type I collagen and bone sialoprotein mRNA during 3D osteogenic culture of ADSC/microsphere composites. Finally, 3D dynamic osteogenic culture generated highly mineralized micro tissues as validated by alizarin red-S staining and SEM-EDS. The results demonstrated that cell-based 3D micro-mineralized tissue could be generated by integrated bioprocess, and potentially utilized for bone tissue regeneration. The integrated bioprocess in this study may provide an efficient and scalable culture system for application in bone tissue engineering.

Keywords: adipose-derived stem cell (ADSC), microsphere, bioreactor, osteogenic, mineralization, micro-tissue.

Introduction

Recently, various somatic stem cells and biomaterials have been developed and clinically applied to restore bone defects, and many efforts to develop *in vitro* three-dimensional (3D) bone tissue-like constructs prior to transplantation. Recently, in the field of bone tissue engineering, bone tissue-like construct has been fabricated by combining stem cell including bone marrow-derived stromal cell (BMSC) and adipose tissue-derived stem cell (ADSC) with various 3D scaffolds which are made of natural or synthetic biomaterials in bench top scale.[1,2] For *in vitro* 3D tissue formation, various scaffolds with porous structure have been designed to support 3D cell growth and differentiation of stem cells, and proper culture system is also essential with suitably designed scaffold. Thus, 2D static culture condition does not provide suitable culture environment for homogenous 3D tissue formation, and cell growth and tissue formation are usually confined on top of surface of scaffold.[3,4] It was reported that higher concentration of nutrient at outer surface of scaffold resulted in the migration of cells which were initially seeded at internal part of the 3D porous scaffold towards that surface *via* chemotaxis, and the remaining cells inside of scaffold showed reduced expression of osteogenic specific genes.[5] It has been also reported that transport of nutrient through 3D scaffold *via* diffusion might not satisfy the metabolic requirement of cells which reside at the center point of 3D scaffold for long culture period.[6] Therefore, for efficient *in vitro* 3D tissue formation, bioreactors have been utilized to facilitate mass transport of nutrient and differentiation-inducing supplements with respect to the supply of oxygen and medium components. In recent years, among various types of bioreactors, rotating wall vessel (RWV) bioreactors have been widely used in cell-based 3D bone tissue formation *in vitro*.[7-9] The RWV bioreactor was designed to optimize to produce laminar flow and minimize the shear stresses and turbulence on cells in 3D culture, providing adequate nutrition and oxygenation, ideal for mammalian cell culture that supports 3D tissue growth.[10] The suspension culture environment of microcarrier in RWV bioreactor is established by the balance between the free falling of the microcarrier inside the bioreactor as a result of gravity and the centrifugal forces due to the rotation of vessels.[10,11]

Accompanied with bioreactor system, another important

*Corresponding Author. E-mail: yshwang@khu.ac.kr

factor in 3D culture system is the selection of microcarrier for cell growth and 3D tissue formation. In bone tissue engineering, various biomaterials such as natural or synthetic polymers and ceramics have been used as supporting template for 3D cell growth and osteogenic differentiation of stem cells. For instance, porous beta tricalcium phosphate (β-TCP) ceramic scaffold was reported to provide spatial growth of bone marrow-derived osteoblasts in perfusion culture system, and the subsequent implantation of the subcultured cell/β-TCP composites aided in forming bone tissue through pores within the scaffold.[12] Such 3D scaffold material could provide a template for spatial growth of cells to achieve the desired form of 3D tissue *in vitro* and *in vivo*. However, even though scaffold materials have highly porous structure for 3D tissue formation, the shape of scaffold might be one of factors which should be considered due to the motion mechanism of scaffold within bioreactor. Studies about simulation and experimental validation of such particle motion in bioreactors to optimize suspension culture have been done.[11,12] Non-homogenous shape like cylindrical or disc type may give rise to very complex motion in rotating bioreactors, which could be very difficult to model and evaluate the influence of mechanical stress to the scaffolds, resulting in poor consistency in data. In contrast, porous scaffold with spherical shape could make it easier relatively to expect and evaluate their motion and the effect of environmental condition in bioreactors. Therefore, the selection of porous 3D scaffolds with adequate shape and bioreactor culture system and their integration are essential to generate *in vitro* 3D cell based tissue engineered construct.

In this study, bioprocess to develop stem cell-based 3D mineralized tissue was designed by integrating ADSCs, porous PLGA microspheres and a high-aspect ratio vessel (HARV) bioreactor as illustrated in Figure 1. First, porous PLGA microspheres were fabricated by a water-in-oil-in-water (W_1/O/W_2) double emulsion method, and surface of microspheres were treated with various molecules to improve initial cell adhesion. After ADSC adhesion in PLGA microspheres, the ADSC/PLGA microspheres were transferred to vessels of a HARV bioreactor, and finally develop *in vitro* 3D bone tissue-like mineralized construct under 3D dynamic osteogenic culture condition, resulting in efficient and reproducible culture system for bone tissue engineering applications.

Experimental

Materials. 50:50 poly(*D*,*L*-lactide-*co*-glycolide) (PLGA) was purchased from the Lakeshore Biomaterials™ (USA). Polyvinyl alcohol (PVA, 87-89% hydrolyzed, Mw 31,000-50,000) was purchased from Sigma (USA). Human Adipose-Derived Stem Cell (ADSC), MesenPRO RS™ Medium supplemented with MesenPRO RS™ Growth Supplement, alpha-minimum essential medium (α-MEM), fetal bovine serum (FBS), phosphate-buffered saline (PBS), trypsin-EDTA and penicillin-streptomycin (PS) were purchased from Invitrogen (USA). All cell culture plastics were purchased from Thermo Finnigan (USA). All other chemicals and regents were of analytical grade.

Preparation of Macroporous PLGA Microsphere and Scanning Electron Microscopic Observation. Macroporous Microspheres were fabricated by a W_1/O/W_2 double-emulsion method, as described in[13] with slight adaptation. A

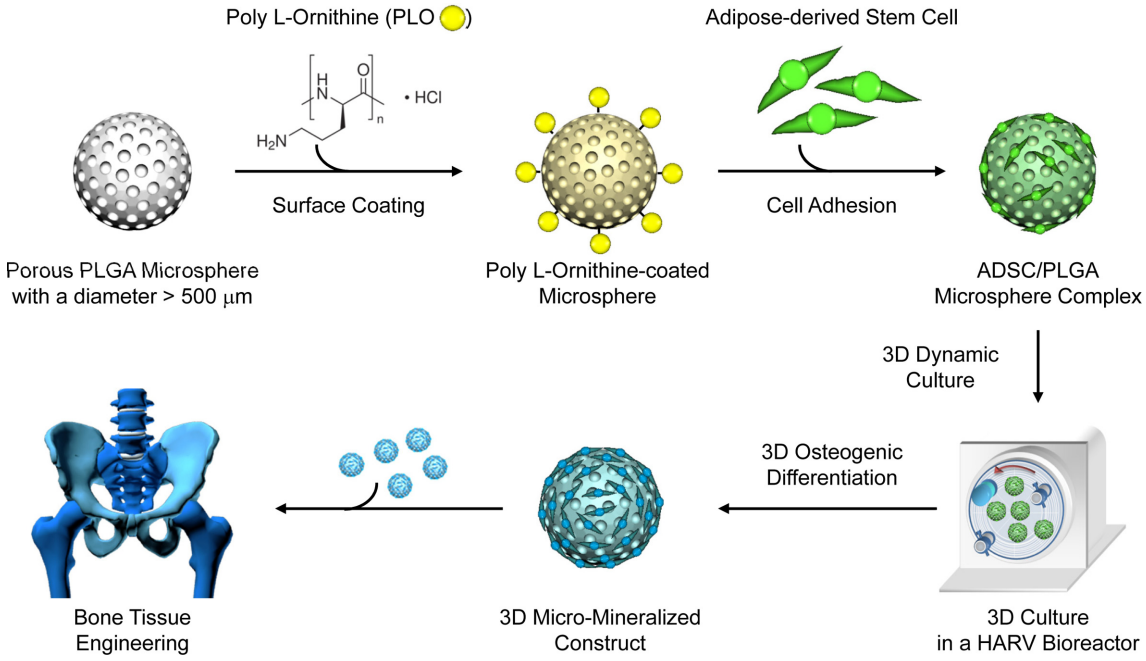

Figure 1. Schematic diagram of integrated bioprocess to develop 3D micro cell-based mineralized tissue.

solution of 62.5 mg/mL PLGA was dissolved in methylene chloride and then mixed with a solution of 210 mg/mL NH_4HCO_3 (Sigma, USA) dissolved in deionized water using a homogenizer (T 25 basic Ultra-Turrax, IKA® Werke GmbH & Co., Germany) at 6,500 rpm for 5 min. This mixture was immediately dropped into a container containing 300 mL of 0.1% (w/v) PVA solution at 10, 20, 30, 40, and 50 cm of drop height and then was re-emulsified using an overhead propeller (PL Techno, Korea) for 4 h at 200 rpm. After the solvent evaporation, the formed microspheres were separated by centrifugation at 3,000 rpm and washed with distilled water five times followed by lyophilization in a freeze dryer for 24 h.

After the microsphere fabrication, the surface and internal structure of formed porous PLGA microspheres was observed by scanning electron microscopy (SEM) (Hitachi S-2300, Hitachi Co. Ltd., Japan). Briefly, dried porous microspheres were frozen and desiccated thoroughly. Then the samples were mounted on a metal stub and coated with platinum using a sputter-coater (IB-3, Giko Engineering Co., Japan) operated at 15 kV for 5 min. The size distribution and the average diameter of microspheres were determined by image analysis (Eyeview Analyzer ver.5.0, Digiplus, Korea, n= 200~250).

Surface Modification of Porous PLGA Microsphere and X-Ray Photoelectron Spectroscopic Analysis. The fabricated macroporous PLGA microspheres were coated with various materials such as FBS (Invitrogen), poly-*L*-ornithine (PLO; mol wt 30,000-70,000; Sigma) or poly-*L*-lysine (PLL; mol wt 30,000-70,000; Sigma) to enhance cell adhesion, and the atomic chemical composition of PLGA surfaces was analyzed with X-ray photoelectron spectroscopy (XPS, K-Alpha, Thermo electron, USA). The microspheres were treated with FBS, 10 μg/mL PLO in PBS or 10 μg/mL PLL in PBS for 24 h at 4 °C for coating, and the coated microspheres were air-dried for 24 h after brief washing with PBS. The coated microspheres were used for cell adhesion assay. For X-ray photoelectron spectroscopic analysis, PLGA films were prepared by casting 62.5 mg/mL PLGA solution on cleaned glass slides, and solvent was evaporated slowly at room temperature for 48 h and then the samples were dried under vacuum at 30 °C for 24 h. The fabricated PLGA films were coated with FBS, 10 μg/mL PLO in PBS or 10 μg/mL PLL in PBS under same condition as the coating procedure of porous PLGA microsphere, and the chemical composition of coated PLGA films were analyzed by XPS.

ADSC Adhesion on Surface Modified Macroporous PLGA Microsphere. Prior to ADSC adhesion, ADSCs were maintained in MesenPRO RS™ Medium supplemented with MesenPRO RS™ Growth Supplement, 2% FBS and 2 mM glutamine. ADSCs were seeded on non-coated, FBS-coated, PLO-coated and PLL-coated macroporous PLGA microspheres at a seeding density of 2.0×10^6 cells/500 microspheres, and cells were allowed to settle on various microspheres for 6, 12, and 24 h in MesenPRO RS™ Medium. After adhesion, unattached cells from ADSC/PLGA microspheres were rinsed with PBS, and then cell adhesion assay was done using Cell Counting Kit (CCK-8) (Dojindo, Japan). After 2 h of incubation with CCK-8 solution, the solutions were transferred to a 96-transwell plate, and the intensity was measured using a microplate reader (BioRad, USA) at a wavelength of 450 nm. The value of intensity was enumerated to relative cell number from a calibration curve generated using the culture of serial number of cells and CCK-8 kit. In addition, cell viability was evaluated using calcein-AM/ethidium homodimer-1 (EthD-1) live/dead assay kit (Invitrogen). In brief, after ADSC adhesion, unattached cells from ADSC/PLGA microspheres were rinsed with PBS, and calcein AM and EthyD-1 were diluted with PBS and added to each ADSC/PLGA microsphere composite according to manufacturer's instruction. After the reaction, the ADSC/microsphere composite was observed using an inverted fluorescence microscope (Olympus IX71Japan).

Osteogenic Differentiation under Static and Dynamic Culture Condition. ADSCs (Passage# 4) were seeded on PLO-coated porous PLGA microspheres at a seeding density of 2.0×10^6 cells/500 microspheres, and were incubated in a 50 mL polypropylene round tube with gentle shaking in MesenPRO RS™ Medium supplemented with MesenPRO RS™ Growth Supplement, 2% FBS and 2 mM glutamine. After 2 h of incubation, unattached cells were removed, and the ADSC/microsphere composites were incubated in the 50 mL polypropylene tube for 24 h. After the incubation, ADSC/Microspheres (50 microspheres/mL) were transferred into 6-well culture plates for static osteogenic culture, and transferred into 10 mL HARV bioreactor vessels for dynamic osteogenic culture. In dynamic osteogenic culture using a HARV bioreactor, each vessel containing ADSC/PLGA composites was rotated anticlockwise at 15 rpm throughout the whole culture period. Osteogenic differentiation in both static and dynamic culture was induced under osteogenic medium; alpha-MEM supplemented with 15% FBS, 10 mM β-glycerol phosphate (Sigma), 0.1 μM dexamethasone (Sigma), and 300 μM ascorbic acid (Sigma). The ADSC/microspheres were cultured in a humidified atmosphere at 37 °C and 5% CO_2 for 4 weeks, and osteogenic medium was refreshed every two days.

Cell Viability Assay. The cell viability of ADSC/microsphere composite in static and dynamic osteogenic culture was evaluated at 0, 7, 14, 21, and 28 days of culture. The ADSC/microspheres composites collected from static and dynamic culture and were washed briefly with PBS and cell viability was evaluated using calcein-AM/EthD-1 live/dead assay kit as previously described. In addition, the viable cell number of ADSC/microsphere composites was evaluated using CCK-8 kit as previously described after 0, 14, and 28 days of 3D dynamic osteogenic culture.

Alkaline Phosphatase (ALPase) Activity Assay. ALPase

activity of ADSC/microsphere composites during 3D dynamic osteogenic differentiation was evaluated. After 0, 7, 14, and 28 days of 3D dynamic osteogenic culture in a HARV Bioreactor, ADSC/microsphere composites were collected from vessels of a HARV bioreactor and washed with PBS. Samples were then diluted using 1x RIPA buffer (50 mM Tri-HCl (pH 7.4), 150 mM NaCl, 0.25% deoxycholic acid, 1% NP-40, and 1 mM EDTA), and a protease inhibitor cocktail (Boehringer Mannheim GmbH, Germany). The cells in ADSC/microsphere composites were lysed in RIPA buffer for 30 min in ice. Each of the lysates was centrifuged at 1,000 rpm at 4 °C for 15 min to remove the cell debris. After centrifugation, the supernatant was collected and then reacted with p-nitrophenyl phosphate solution (PNPP, Sigma) for 30 min in a 5% CO_2 humidified incubator at 37 °C. The reaction with PNPP was then terminated by adding 50 μL of 1 N NaOH. The production of p-nitrophenol was determined by absorption at 405 nm using a microplate reader. A calibration curve was generated using standard *p*-nitrophenol solution (Sigma) and the amount of total *p*-nitrophenol produced from cultured cells was enumerated from the calibration curve. Finally, the enzyme activity (n=4 per group) was expressed as micromoles of reaction product (*p*-nitrophenol) per minute per mg of total cellular protein.

Quantitative Real-Time Polymerase Chain Reaction (Real-time qPCR) Analysis. After 0, 7, 14, and 28 days of 3D osteogenic culture in a HARV bioreactor, ADSC/microsphere composites were collected from vessels of a HARV bioreactor, and total RNA was isolated from ADSC/microsphere composites using Trizol reagent (Invitrogen). Isolated RNA was treated with DNase I (Invitrogen), and then reverse-transcription reactions were performed using SuperScript III (Invitrogen) following the manufacturer's instruction. 2 μg of total RNA was used for each cDNA synthesis. Measurements of cDNA levels were performed by quantitative RT-PCR using a Bio-Rad CFX96 detection system and an iQ SYBR green supermix (Bio-Rad) fluorescence. Samples were subjected to the following conditions in an ExiCycler: initial denaturation at 94 °C for 10 min followed by 45 cycles of 94 °C for 40 s, 58 °C for 30 s, and 72 °C for 30 s. Relative quantification was calculated using the 2-delta delta ct (cycle-threshold) method. To confirm the amplification of specific transcripts, melting curve profiles were produced at the end of each PCR by cooling the sample to 40 °C and then heating it slowly to 95 °C while continuously measuring the fluorescence. PCR reactions were performed using the following bone-specific primers: Runx2 (runt-related transcription factor), SP7 (Osterix), BSP (Bone sialoprotein), Col 1 (type I collagen) and GAPDH were measured by real-time PCR in an ExiCycler (Bioneer, Korea). Each primers were pre-desigened for real-time PCR and purchased from Bioneer. All real-time qPCR results were normalized by GAPDH.

Alizarin Red S (ARS)-Staining and Immunohistochemical Staining. For ARS and immunohistochemical staining, ADSC/microsphere composites were collected from HARV bioreactor vessels after 28 days of 3D osteogenic culture. The ADSC/microsphere composites were fixed in 3.7% formaldehyde at 4 °C for 24 h. Fixed ADSC/microsphere composites were dehydrated by placing in a sequential series of increasing ethanol concentrations to remove all the water. The ethanol was then completely replaced with sequential series of increasing xylene concentration until 100% xylene followed by incubation with paraffin saturated xylene at room temperature overnight. The composites in paraffin saturated xylene were then placed in an oven (60 °C) for 20 min. The xylene was then completely replaced with pre-warmed liquid paraffin. The composites were then serially sectioned (5 μm) and left at room temperature overnight to adhere to Vectabonded™ (Vector Laboratories, USA) glass slides. For staining, the paraffin was completely removed from the sections by immersion in xylene, decreasing ethanol concentrations and then by washing with tap water. For immunostaining, the deparaffinised sections were antigen-retrieved by microwave pretreatment in citrate buffer (pH 6.0) and allowed to cool to retrieve the antigens. The sections of ADSC/microsphere composites were immersed in a 2% (w/v) Alizarin Red S (ARS, Sigma) solution (pH 4.2) for 5 min at room temperature, and excessive staining was washed in tap water and rinsed once in distilled water. The slides were examined using an inverted fluorescence microscope (Olympus IX71). In addition, the sections of ADSC/microsphere composites cells were permeabilized with 0.2% Triton X-100 (Sigma) for 20 min, and blocked with 4% bovine serum albumin (BSA) solution in PBS. After 1 h of blocking at room temperature, sections were reacted with primary antibodies at 4 °C for overnight and secondary antibodies at room temperature for 1 h. Dilution rate of primary antibodies in 1% BSA solution as follows: type I collagen (mouse monoclonal, 1:500; Santa Cruz, Germany), osteocalcin (OCN) (mouse monoclonal, 1:500; Santa Cruz, Germany), and Runt-related transcription factor 2 (Runx2) (mouse monoclonal, 1:1000; AbCam, USA). Dilution rate of secondary antibodies in 1% BSA solution as follows: 1:2000 anti-mouse IgG-alexa 488 (Invitrogen, USA) and 1:2000 anti-mouse IgG-alexa 596 (Invitrogen, USA). Finally, the sections were washed with PBS and counter-stained with 4',6-diamidino-2-phenylindole dihydrochloride (DAPI). Fluorescently labeled tissue was imaged using an inverted fluorescence microscopy.

Scanning Electron Microscope - Energy Dispersive X-Ray Spectroscopy (SEM-EDS) Analysis. The mineralized surface of ADSC/microsphere composites was observed by scanning electron microscopy (SEM) (Hitachi S-230, Japan) after 28 days of 3D dynamic osteogenic culture in a HARV bioreactor. Briefly, the ADSC/microsphere composites were fixed with 3% glutaraldehyde for 24 h, and then freeze-dried. Samples were mounted and sputter-coated with gold using an ion coater and observed at an accelerating voltage of 20 kV. In order to characterize the morphology and the

chemical composition of the mineralized nodules within the hydrogels, energy dispersive X-ray (EDS) analysis was carried out with a LEO Gemini Field Emission Gun-Scanning Electron Microscope (FEG-SEM, Carl Zeiss, UK).

Statistical Analysis. A one-way ANOVA was used to analyze the mechanical analysis results ($p<0.05$).

Results and Discussion

Fabrication and Surface Modification of Macroporous PLGA microspheres and Cell Adhesion. Highly open porous biodegradable PLGA microspheres were fabricated by using a water-in-oil-in-water ($W_1/O/W_2$) double emulsion method, and the drop height-dependent size of porous microsphere and porous structure were evaluated (Figure 2(A)). Ammonium bicarbonate was dissolved in the inner W_1 droplets as a gas foaming agent, and the oil phase was methylene chloride containing PLGA. The dissolved ammonium bicarbonate in the W_1 droplets generated gas bubbles upon contact with the primary W_1/O emulsion with W_2 phase, there by stabilizing the emulsion and creating open porous morphology throughout the PLGA microspheres. The size and porosity of microsphere was dependent on height of droplets, and size distribution and morphology of the formed PLGA microspheres are shown in Figure 2. First, the average size of macroporous PLGA microspheres was controllable by the drop height, and the size of microspheres increased as the drop height increased. The average diameter of porous PLGA microspheres was approximately 474, 593, 622, 731 and 729 μm for 10, 20, 30, 40 and 50 cm of drop height, respectively (Figure 2(B)). Above the 40 cm drop height, the microsphere no longer increased. In addition to size variation, the porosity and spherical structure of microsphere were also influenced by drop height. As shown in SEM images (Figure 2(C)), with increasing drop height, the porosity of microsphere also increased. At drop height of 10 and 20 cm, the porosity and the lack of inter-connection between pores were observed, and the shape of microspheres was found to

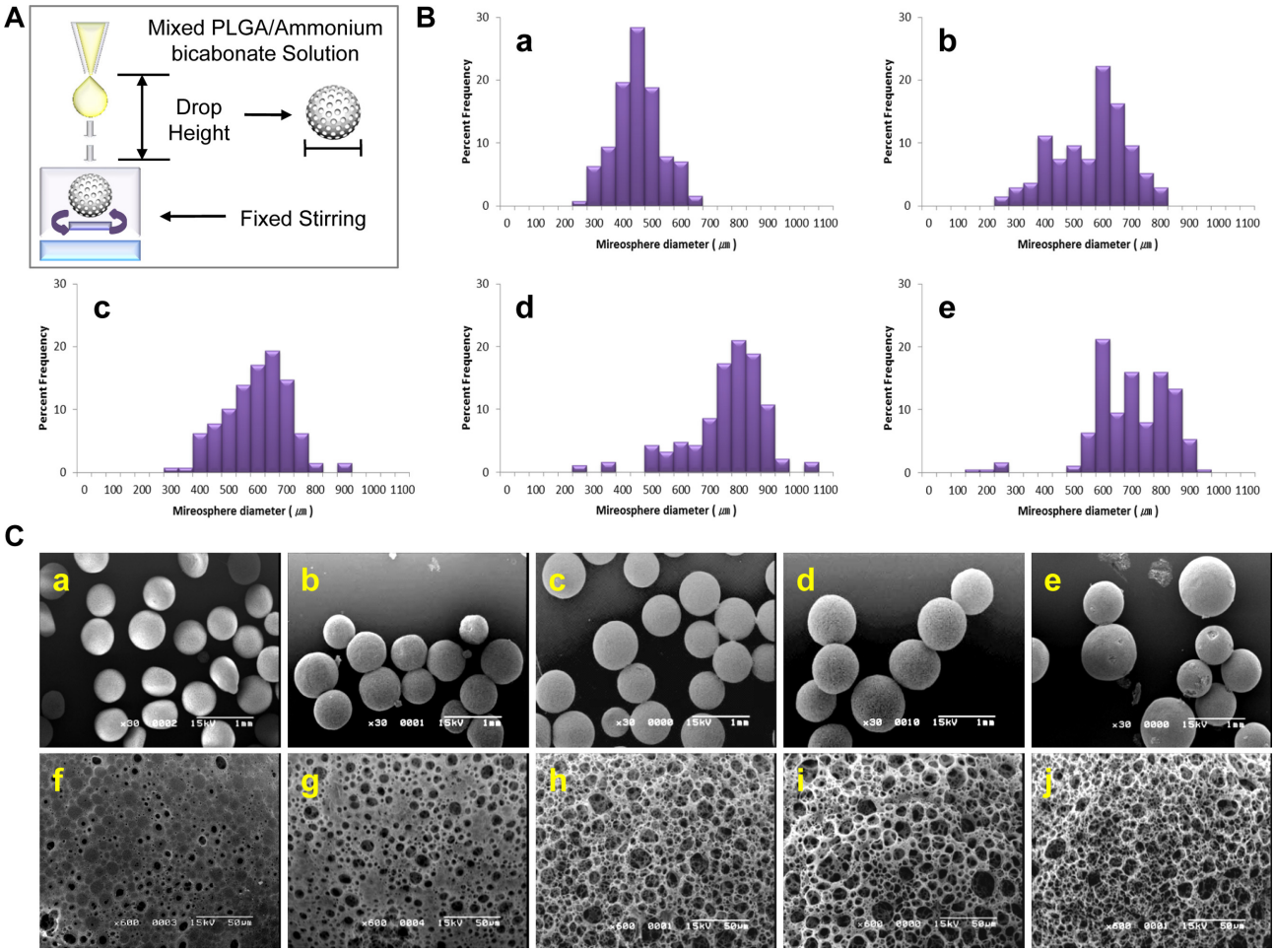

Figure 2. The size distribution and surface morphology of macroporous PLGA microspheres. (A) Schematic diagram of PLGA microsphere fabrication. (B) Size distribution of porous PLGA microsphere according to different drop heights: (a) 10, (b) 20, (c) 30, (d) 40, and (e) 50 cm. (C) Surface morphologies of the formed PLGA microspheres according to different drop height (SEM image): (a),(f) 10 cm, (b),(g) 20 cm, (c),(h) 30 cm, (d),(i) 40 cm, and (e),(j) 50 cm.

be irregular. In contrast, above 30 cm of drop height, the formed microspheres showed large open pores on the surface with diameter size above 20 μm with the existence of a binary pore distribution composed of small and large pores, sufficient for cell growth and infiltration finally to form 3D tissue.

Following the evaluation of the size distribution and the formation of pore structure in PLGA microsphere, macroporous PLGA microspheres with approximately 800 μm of a diameter were fabricated by dropping at 40 cm of height using $W_1/O/W_2$ double emulsion method, and then were coated with various adhesion inducing materials such as PLL and PLO to further improve initial cell adhesion on the surface of porous PLGA microsphere. For XPS analysis, various materials-coated PLGA films were fabricated under same condition with porous PLGA microsphere. The XPS spectra showed the corresponding regions of the spectrum about O 1s, C 1s, and N 1s for non-coated, PLL-coated and PLO-coated PLGA films. As shown in Figure 3(A), carbon and oxygen was detected on all samples, but nitrogen peak was only detectable in PLL-coated and PLO-coated PLGA films. The atomic percentage for PLL-coated and PLO-coated PLGA film was calculated and shown in Figure 3(A)(c), and the content of nitrogen was 0.63 and 0.92 wt% in PLO-coated PLGA film and PLL-coated PLGA film, which indicated the existence of nitrogen atom from the coated PLO and PLL.

After surface-modification of the fabricated macroporous PLGA microsphere, the adhesion activity of ADSC was evaluated for non-coated, FBS-coated, PLL-coated and PLO-coated porous PLGA microspheres (Figure 3(B) and (C)). Significantly higher adhesion activity of ADSCs was found in ADSC culture on PLL-coated and PLO-coated microspheres after 6, 12, and 24 h of seeding. PLO-coated microspheres showed the highest cell adhesion even after 6 h of seeding. Relatively higher cell adhesion was found in FBS-coated microspheres in comparison with non-coated micro-

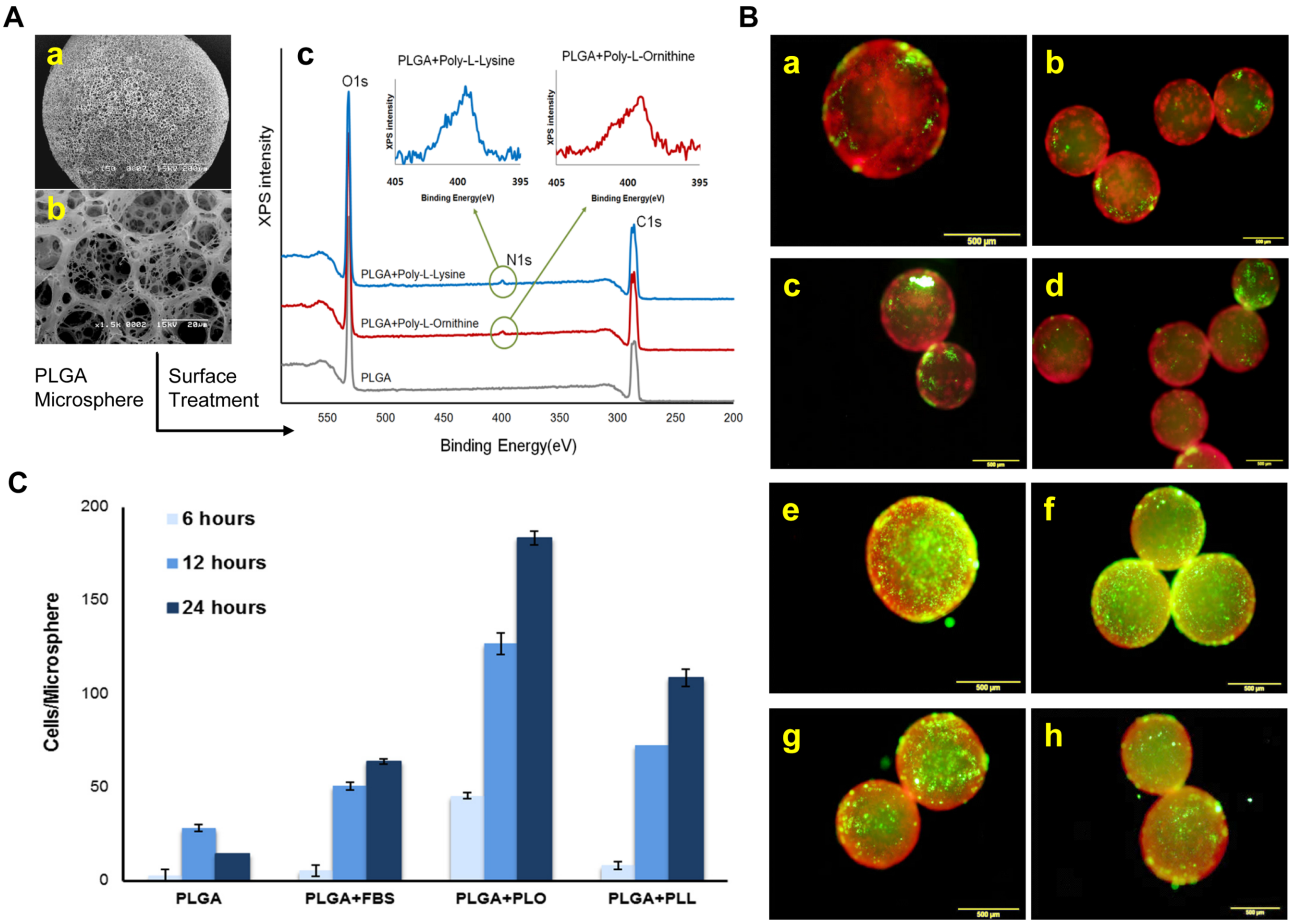

Figure 3. XPS analysis of surface-modified porous PLGA microspheres and ADSC adhesion on surface-modified porous PLGA microspheres. (A) XPS analysis of surface-modified porous PLGA microspheres: (a),(b) SEM images of surface-modifed porous PLGA microspheres with above 800 μm of a diameter. (c) XPS analysis of PLO- or PLL-coated PLGA substrate. (B) Live/Dead assay of adhered ADSCs on various materials-coated porous PLGA microspheres after 24 h of seeding: (a),(b) non-coated, (c),(d) FBS-coated, (e),(f) PLO-coated, and (g),(h) PLO-coated. (C) The adhesion activity of ADSC was evaluated for non-coated, FBS-coated, PLL-coated, and PLO-coated porous PLGA microspheres on the surface after 6, 12, and 24 h of seeding.

sphere, but much lower cell adhesion activity was observed in comparison with PLL-coated and PLO-coated macroporous PLGA microspheres. In addition, some smears indicating cell detachment were found on the surface of non-coated and FBS-coated PLGA microspheres, which might be due to weak cell adhesion and washing-out during brief washing process before live/dead assay. In consistent with cell adhesion assay, higher number of viable cells was found to adhere homogenously onto the surface of PLO-coated porous PLGA microspheres, which indicated PLO coating provided most favorable surface for cell adhesion in comparison with other tested coating materials. From the results of physicochemical characterization and cell adhesion, PLO-coated macrophorous PLGA microsphere with approximate 800 μm of a diameter was selected to use as supporting matrix for 3D micro-tissue formation.

***In vitro* 3D Micro-Mineralized Tissue Formation by 3D Dynamic Culture in a HARV Bioreactor.** After cell adhesion on PLO-coated macroporous PLGA microspheres, the ADSC/microsphere composites were allowed to form 3D micro-mineralized tissue under static and dynamic culture environment in the presence of osteogenic supplements such as ascorbic acid, glycerophosphate and dexamethasone. When the composites were placed and cultured in 6 well culture plates as static culture, the attached viable cells on microspheres were observed after 1 week of osteogenic culture. However, poor cell growth and large cell loss on the surface of microshperes was found in 2 weeks of culture, and agglomeration between ADSC/microsphere composites was frequently observed (Figure 4(A)(a,b,e,f)). In contrast, when the composites were cultured in suspension within a HARV bioreactor, cells proliferated and viable cells covered all surface area of microspheres. In addition, after prolonged cultivation of 2 and 4 weeks under 3D dynamic culture condition, we observed complete spreading of cells on the surface with spindle shapes (Figure 4(A)(c,d,g,h,i). The number of cells on a porous PLGA microsphere increased almost 26 folds, approximately from 121 at day 0 to 3137 at day 28 (Figure 4(B)).

After 4 weeks of osteogenic culture under 3D dynamic culture condition, as shown in SEM picture (Figure 5(A)), adhered cells were well grown, and high contents of mineral deposits were formed on macroporous PLGA microsphere. ARS staining of the sectioned cell/microsphere composites showed highly calcium-based mineral deposits on multi-cell layers formed in porous microspheres (Figure 5(B)). Chemical composition of the mineral deposits formed on cell/microsphere composite was characterized by SEM-EDS, which

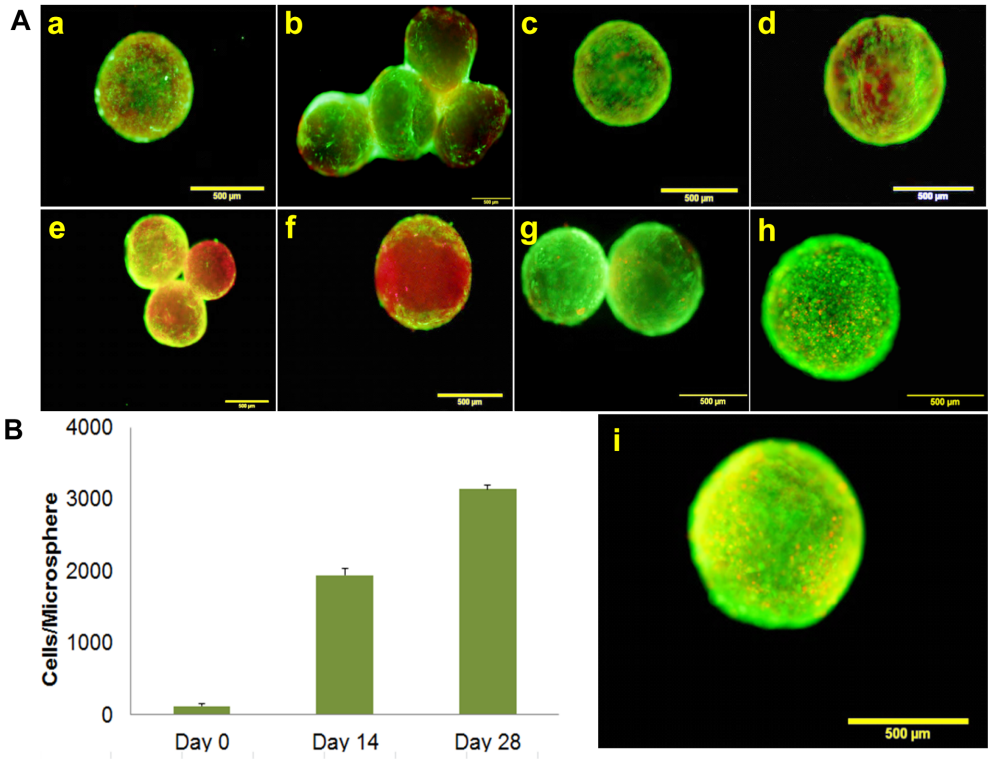

Figure 4. Live/dead assay and cell growth assay of ADSCs/microsphere composite culture under static and 3D dynamic conditions. (A) Live/dead assay for ADSCs/microsphere composite under static and dynamic culture conditions: (a),(b) Static culture for 1 week, (c),(d) dynamic culture for 1 week, (e),(f) static culture for 2 weeks, (g),(h) dynamic culture for 2 weeks, and (i) dynamic culture for 4 weeks. (B) ADSC proliferation on porous PLGA microsphere in the culture within a HARV bioreactor.

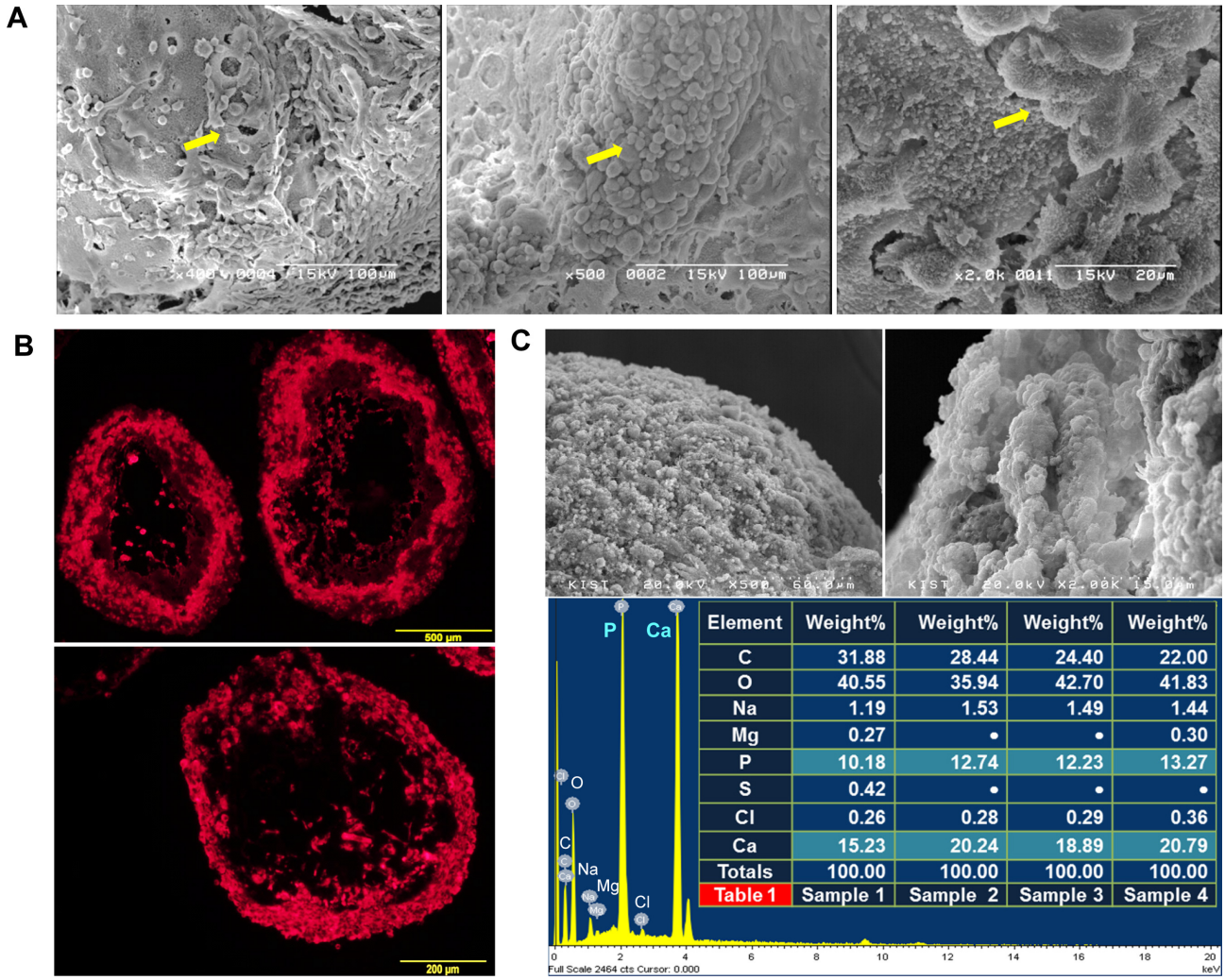

Figure 5. Mineralization of ADSC/microsphere composite after 3D dynamic osteogenic culture. (A) SEM Images of ADSC and mineral deposits on surface of ADSC/microsphere composite after 4 weeks of 3D dynamic osteogenic culture in a HARV bioreactor. Arrows indicate cells. (B) Alizarin red S staining of ADSC/microsphere composite after 4 weeks of 3D dynamic osteogenic culture in a HARV bioreactor. (C) SEM-EDS analysis of the mineral deposits formed on ADSC/microsphere composite after 4 weeks of 3D dynamic osteogenic culture in a HARV bioreactor.

showed high contents of calcium and phosphorus ion in mineral deposits and 12.11±1.3% and 18.79±2.3% (wt%) in calcium and phosphorus content, and molar ratio of calcium/phosphorus was approximately 1.202 (Figure 5(C)). The mineralization was accompanied with ostegenic differentiation of ADSCs which was induced in the presence of osteogenic supplements in a HARV bioreactor. As shown in Figure 6(A), osteogenic differentiation was characterized by the time dependent-temporal increase of ALPase activity, which is traditional tendency of ALPase activity during osteogenic differentiation. ALPase activity showed gradual increase until 14 days of osteogenic culture and subsequent decrease thereafter. Furthermore, immunocytochemical staining for the section of ADSC/microsphere composite showed strong expression of several osteogenic markers such as type I collagen, OCN and runx2 in multi-cell layers. Figure 6(C) showed distinct expression of type I collagen and OCN around cells expressing runx2 in nucleus. Such molecular expression was proved by gene expression analysis with real-time qPCR. mRNAs of several markers indicating osteogenic differentiation elevated during 3D osteogenic culture (Figure 6(B)). mRNAs of type I collagen and BSP, a major extracellular matrix or protein produced from osteoblast, and sp7, also called osterix, and runx2, one of major transcription factor to modulate osteogenic differentiation, were upregulated during whole osteogenic culture period, and especially all expressions of evaluated genes were dramatically increased from day 14 of 3D osteogenic culture. From these results, highly mineralized micro tissue formation was proved to be accompanied with differentiation of ADSC on macroporous PLGA

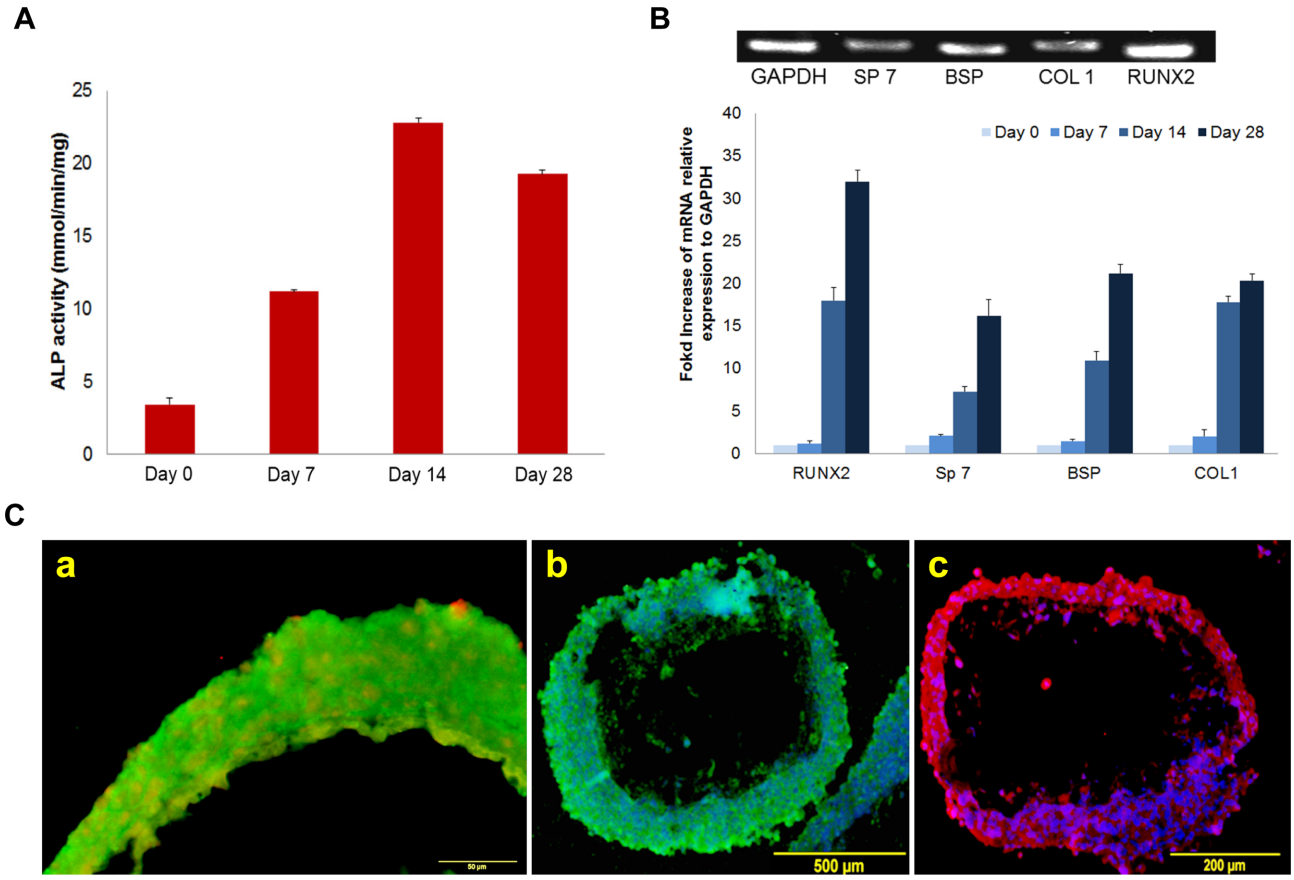

Figure 6. Characterization of 3D osteogenic differentiation. (A) ALPase activity assay, (B) RT-PCR and real-time qPCR analysis, (C) immunofluorescence images of ADSC/microsphere composite after 4 weeks of 3D dynamic osteogenic culture in a HARV bioreactor: (a) type I collagen (green) and runx2 2 (red), (b) type I collagen I (green) counter stain with DAPI (blue), (c) OCN (red) counter stain with DAPI (blue).

microsphere towards osteogenic lineage.

Bone defects result in pain and disability for millions of people worldwide, and bone tissue restoration has received significant interest in regenerative medicine. To date, autologous and allogenous bone graft have been widely accepted as one of the most effective way to restore defected bone tissue, but challenges still remain. For instance, cell therapy has been suggested as an effective alternative for patients with osteoporosis, but this has not been widely accepted for clinical practice due to the shortage of donor cells.[14] Recently, stem cell-based approaches have been considered as an alternative strategy to regenerate defected bone tissue, and extensive stem cell research showed successful generation of osteoblast from adult stem cells such as BMSC and ADSC, which might provide clinically available potent cell source. In addition, along with adult stem cell research, regenerative bone tissue engineering-based approach has been emerged as one effective way to produce functional mineralized tissues that can be used to restore damaged bone tissues. In general, bone tissue engineering progress includes methods for the harvest, expansion, osteogenic differentiation of stem cells and transplantation of tissue-forming cells, the use of bioactive matrix materials to support spatial growth and 3D tissue formation, local or systemic delivery of various hormones and growth factors or other chemical compounds, and other methods to control the culture environment.[15-17] To date, there has been significant progress in developing tissue engineered bone constructs using various scaffolds and cells. For instance, in bone tissue engineering, many suitable materials have been generated, including synthetic calcium phosphate-based ceramics and polyglycolic and polylactic acids. Synthetic polymeric scaffold composed of polylactic acid or poly(*L*-lactic) acid natural collagen or tricalcium phosphate ceramics have been used as porous scaffold to provide suitable environment for 3D osteogenic cell growth and function.[12,18,19] Furthermore, accompanied with cells and scaffolds, bioreactors have been used to promote *in vitro* 3D bone tissue formation by providing suspension culture condition for 3D cell growth.[20] For instance, *in vitro* 3D mineralized tissues could be generated from osteogenic culture of mouse embryonic stem cells (mESC) *via* suspension culture in a HARV bioreactor,[9] and the accelerated nutrient con-

sumption by metabolic activity of mESC-based 3D tissue was shown in 3D culture suggesting improved function of a bioreactor for 3D tissue formation. However, the size control of 3D tissues could not be achieved by culturing cell-based tissue only in a rotating bioreactor without proper scaffolds.

In this study, integrated bioprocess to generate stem cell-based microscale mineralized tissue was developed to combine ADSC, porous PLGA microspheres and a HARV bioreactor. First, spherical shaped microscale polymeric scaffold was designed with regards to the motion and the mechanical stress to particles within a rotating bioreactor.[11] Polymeric macroporous microspheres have been developed initially to deliver growth factor,[21] and recently have been used for cell delivery in various fields of tissue engineering.[22-24] Porous PLGA microspheres in this study were fabricated by W1/O/W2 double emulsion method[13] to provide structural support for 3D cell growth and tissue formation. The porosity and size of microspheres could be easily controlled by the drop height of PLGA solution containing ammonium bicarbonate, and microspheres with diameter above 500 μm was selected to provide sufficient surface area for 3D cell growth. In addition, accompanied with the scaffold material, the cells are important for the production of new tissue through ECM synthesis and are responsible for the long-term stability of this matrix. Addition of a cellular component to the scaffold may aid in repairing tissue at a faster rate as well as in repairing larger defects. Thus, the interaction of scaffolds and cells, cell adhesion on the matrix surface, cell maturation, ECM production, and cell proliferation are all important for the success of a tissue engineered bone construct. In this study, the surface of porous PLGA scaffold was coated with FBS, PLL, and PLO to facilitate the interaction of stem cells and polymeric scaffold at initial cell adhesion process, and adhesion and live/dead assay showed most effective adhesion activity for microsphere coated with PLO. Although biological mechanism for adhesive interaction between PLO and cell has not been well elucidated, it was reported that focal adhesions were found in cells plated on PLO coated substrate and this interaction might be driven by self-adhesion to the endogenously produced adhesion molecule such as fibronectin, following initial interaction of cells to charged PLO substrate.[25] However, the efficacy of cell adhesion even on PLO coated microspheres was approximately 20% (200 cells/microsphere) of initial cell seeding density (4,000 cells/microsphere) and still low, which should be overcome and need to be studied further to improve cell adhesion efficacy.

In next bioprocess, the cell/microsphere composites were transferred to vessels of a HARV bioreactor, and were cultured in the presence of osteogenic supplements such as ascorbic acid, glycerophosphate and dexamethasone. In 3D dynamic culture in a HARV bioreactor, cells proliferated, metabolically viable and covered all surface area of porous PLGA microsphere after 4 weeks of osteogenic culture validated by proliferation, live/dead assay and SEM analysis. In contrast, in 2D static culture, viable cells could be hardly observed on the surface of porous PLGA microsphere even after 2 weeks of osteogenic culture, which might be related to poor cell growth due to limited mass-transport of nutrient in static culture condition[6] and cell loss due to certain physical contact to surface of well culture plate during inevitable experimental handling such as spontaneous settle-down of cell/scaffold composite due to gravity and media refreshment. These results represent 3D dynamic culture condition accompanied with 3D spherical scaffold is essential to facilitate nutrient transport and support well homogenous 3D cell growth to form tissue *in vitro*. Furthermore, the 3D tissue engineered construct was allowed to form mineralized tissue *via* osteogenic differentiation of ADSC in the presence of osteogenic supplements such as ascorbic acid, glycerophosphate and dexamethasone.[26] 3D dynamic osteogenic culture generated highly mineralized tissue, and Alizarin red-S staining and SEM-EDS analysis showed high deposition of calcium/phosphate-based minerals on the cell surface of cell/microsphere composites. Bone is a highly mineralized hard tissue, and the hard matrix is mainly composed of calcium/phosphate-based minerals deposited around protein fibers such as collagen.[27] Type I collagen was highly expressed in multi-layered runx2, one of major transcription factors to be expressed during osteogenic differentiation and participates in osteoblast maturation by controlling the expression of type I collagen and bone sialoproteins such as osteocalcin,[28,29] -expressing cells in cell/microsphere composites. Osteocalcin, a highly phosphorylated sialoprotein that is induced with the onset of mineralization at late stages of differentiation,[30] expression was also found through whole area of the composites. As shown in histological and immunohistological staining, the void area within the sectioned tissue construct could be observed. Such void volume within mineralized tissue construct might not be due to PLGA degradation during 4 weeks of dynamic culture. Although the degradation rate of PLGA depends on size, shape, porosity, molecular weight and the condition of culture, it has been well reported that 50/50 PLGA microsphere could be degraded *in vitro* at above 60 days of incubation.[31] In addition, the void volume within porous PLGA microsphere is reported to be formed during fabrication process using a $W_1/O/W_2$ double-emulsion method.[13] The mineralized tissue formation was accompanied with osteogenic differentiation of ADSC on porous PLGA microsphere. ALPase is known to initiate biological mineralization by hydrolyzing β-glycerophosphate and promoting mineralization.[32] The temporal increase of ALPase activity observed in our results is consistent with the progress of mineralization during osteogenic differentiation.[33] Consistent with temporal increase of ALPase, mRNA expression of several markers such as type I collagen, runx2, BSP and sp7, also named osterix and an osteoblast-specific transcription factor, were upregulated in

accordance with culture time indicating osteogenic differentiation of ADSC.

Conclusions

In this study, our proposed integrated bioprocess was composed by the fabrication of size controllable polymeric porous microsphere as supporting matrix for 3D cell and tissue growth, culture condition for osteogenic differentiation of stem cell and dynamic culture system using a HARV bioreactor for the purpose of developing *in vitro* cell-based mineralized tissue. Integrated bioprocess described here would provide an efficient method to develop 3D cell-based micro-mineralized tissue, and has shown potential as an alternative strategy for bone repair and bone tissue engineering. Thus, future research in implantation of the developed 3D cell-based micro-mineralized tissue is essential for further validation of the demonstrated dynamic culture system.

Acknowledgments. This research was supported by grand No. 20110013333, 2012010181, and 2012R1A5A2051387 from the Basic Research Program through the National Research Foundation of Korea (NRF) funded by the Korea government (MEST) and by grand No. A100208 from Korea Health Industry Development Institute, Republic of Korea.

References

(1) F. D. Ceuninck, C. Lesur, P. Pastoureau, A. Caliez, and M. Sabatini, *Methods Mol. Med.*, **100**, 15 (2004).
(2) N. S. Hwang, M. S. Kim, S. Sampattavanich, J. H. Baek, Z. Zhang, and J. Elisseeff, *Stem Cells,* **24**, 284 (2006).
(3) S. L. Ishaug-Riley, G. M. Crane-Kruger, M. J. Yaszemski, and A. G. Mikos, *Biomaterials,* **19**, 1405 (1998).
(4) C. E. Holy, M. S. Shoichet, and J. E. Davies, *J. Biomed. Mater. Res.*, **51**, 376 (2000).
(5) J. Glowacki, S. Mizuno, and J. S. Greenberger, *Cell Transplant.*, **7**, 319 (1998).
(6) S. M. Mueller, S. Mizuno, L. C. Gerstenfeld, and J. Glowacki, *J. Bone Miner. Res.*, **14**, 2118 (1999).
(7) Q. Q. Qiu, P. Ducheyne, and P. S. Ayyaswamy, *Biomaterials,* **20**, 989 (1999).
(8) E. A. Botchwey, S. R. Pollack, E. M. Levine, and C. T. Laurencin, *J. Biomed. Mater. Res.*, **55**, 242 (2001).
(9) Y. S. Hwang, J. Cho, K. L. A. Chan, J. Heng, A. R. Boccacini, S. G. Kazarian, D. Williams, J. M. Polak, and A. Mantalaris, *Biomaterials,* **30**, 499 (2009).
(10) T. G. Hammond and J. M. Hammond, *Am. J. Physiol. Renal. Physiol.*, **281**, 12 (2001).
(11) S. R. Pollack, D. F. Meany, E. M. Levine, M. Litt, and E. D. Johnston, *Tissue Eng.*, **6**, 519 (2000).
(12) Y. Wang, T. Umera, J. Dong, H. Kojima, J. Tanaka, and T. Tateichi, *Tissue Eng.*, **9**, 1205 (2003).
(13) T. K. Kim, J. J. Yoon, D. S. Lee, and T. G. Park, *Biomaterials*, **27**, 152 (2006).
(14) R. R. Betz, *Orthopaedics*, **25**, S561 (2002).
(15) H. Petite, V. Viateau, W. Bensaid, A. Meunier, C. de Pollak, M. Bourguignon, K. Oudina, L. Sedel, and G. Guillemin, *Nat. Biotechnol.*, **18**, 959 (2000).
(16) S. Tamura, H. Kataoka, Y. Matsui, Y. Shionoya, K. Ohno, and K. I. Michi, *Bone,* **29**, 169 (2001).
(17) J. L. B. Karen, P. Scott, and F. K. James, *Biomaterials,* **21**, 2347 (2000).
(18) D. W. Hutmacher, *Biomaterials,* **21**, 2529 (2000).
(19) J. J. Blaker, V. Maquet. R. Jerome, A. R. Boccaccini, and S. N. Nazhat, *Acta Biomater.*, **1**, 643 (2005).
(20) Z. Y. Zhang, S. H. Teoh, E. Y. Teo, M. S. K. Chong, C. W. Shin, F. T. Tien, M. A. Choolani, and J. K. Y. Chan, *Biomaterials,* **31**, 8684 (2010).
(21) H. H. Chung, H. K. Kim, J. J. Yoon, and T. G. Park, *Pharm. Res.*, **23**, 1835 (2006).
(22) C. C. Huang, H. J. Wei, Y. C. Yeh, J. J. Wang, W. W. Lin, T. Y. Lee, S. M. Hwang, S. W. Choi, Y. Xia, Y. Chang, and H. W. Sung, *Biomaterials,* **33**, 4069 (2012).
(23) S. W. Kang, S. W. Seo, C. Y. Choi, and B. S. Kim, *Tissue Eng. Part C*, **14**, 25 (2008).
(24) S. W. Kang, W. G. La, and B. S. Kim, *J. Biomater. Sci.*, **20**, 399 (2009).
(25) M. M. Harper, E. A. Ye, C. C. Blong, M. L. Jacobson, and D. S. Sakaguchi, *J. Mol. Neurosci.*, **40**, 269 (2010).
(26) J. M. Song, B. C. Kim, J. H. Park, I. K. Kwon, A. Mantalaris, and Y. S. Hwang, *Biomed. Mater.*, **5**, 1 (2010).
(27) E. Seeman and P. D. Delmas, *N Engl J.Med,* **354**, 2250 (2006).
(28) P. Ducy, R. Zhang, V. Geoffroy, A. L. Ridall, and G. Karsenty, *Cell,* **89**, 747 (1997).
(29) C. Banerjee, A. Javed, J. Y. Choi, J. Green, V. Rosen, A. J. van Wijnen, J. L. Stein, J. E. Lian, and G. S. Stein, *Endocrinology,* **142**, 4026 (2001).
(30) V. Viereck, H. Siqqelkow, S. Tauber, D. Raddatz, N. Schutze, and M. Hufner, *J. Cell. Biochem.*, **86**, 348 (2002).
(31) M. A. Tracy, K. L. Ward, L. Firouzabadian, Y. Wang, N. Dong, R. Qian, and Y. Zhang, *Biomaterials*, **20**, 1057 (1999).
(32) Y. Sugawara, K. Suzuki, M. Koshikawa, M. Ando, and J. Iida, *Jpn. J. Pharmacol.*, **88**, 262 (2002).
(33) M. Yoshikawa, K. Suzuki, T. Kajii, M. Koshikawa, T. Imai, and A. Matsumoto, *J. Hard Tissue Biol.*, **8**, 37 (1999).